ARTICLES
https://doi.org/10.1038/s41561-017-0035-y
nature geoscience
Corrected: Publisher correction

Western US volcanism due to intruding oceanic mantle driven by ancient Farallon slabs

Quan Zhou*, Lijun Liu and Jiashun Hu

The origin of late Cenozoic intraplate volcanism over the western United States is debated. One important reason is the lack of a clear understanding of the mantle dynamics during this volcanic history. Here we reconstruct the mantle thermal states beneath North America since 20 million years ago using a hybrid inverse geodynamic model with data assimilation. The model simultaneously satisfies the past subduction kinematics, present mantle tomographic image and the volcanic history. We find that volcanism in both the Yellowstone volcanic province and the Basin and Range province corresponds to a similar eastward-intruding mantle derived from beneath the Pacific Ocean and driven mostly by the sinking Farallon slab below the central-eastern United States. The hot mantle that forms the Columbia River flood basalt and subsequent Yellowstone–Newberry hotspot tracks first enters the western United States through tears within the Juan de Fuca slab. Subsequent coexistence of the westward asthenospheric flow above the retreating Juan de Fuca slab and eastward-propagating mantle beyond the back-arc region reproduces the bifurcating hotspot chains. A similar but weaker heat source intrudes below the Basin and Range around the southern edge of the slab, and can explain the diffuse basaltic volcanism in this region. According to our models, the putative Yellowstone plume contributes little to the formation of the Yellowstone volcanic province.

The origin of intraplate volcanism remains a fundamental scientific question. One example is the Yellowstone Volcanic Province (YVP) that includes the mid-Miocene Columbia River flood basalt (CRFB) and the subsequent Yellowstone (YS) and Newberry (NB) hotspot tracks (Fig. 1). These volcanic activities were accompanied by concurrent volcanism within the basin and range (B&R) on the south, which is usually considered mechanically different from the former. These volcanic processes coincided with a complex tectonic history of the western United States, including nearby subduction, crustal extension and sublithospheric convection. Proposed mechanisms for the western US intraplate volcanisms largely fall into two categories: a deep origin that involves a hot mantle plume[1–4], and a shallow origin that includes lithosphere extension[5,6], slab-induced upwelling[7,8] and small-scale convection[9,10].

Besides these models that all concern tectonic events within the region below western United States, another potentially important driving force is the ancient Farallon slab located under the eastern United States. The west coast of North America has experienced continuous subduction since the Mesozoic[11], resulting in a huge volume of accumulated slab beneath the east coast[12–15]. This ancient Farallon slab, with a slow descending rate into the lower mantle[16], actively affects the surface topography over eastern North America[17,18]. However, its influence on the mantle flow beneath the western United States remains unclear.

Indeed, it is the uncertain evolution of mantle dynamics below the western United States that has caused the debates on the formation of the intraplate volcanism. For example, Kincaid et al.[4] suggested that the slab-induced return flow bifurcates the YS plume, which resulted in the YS and NB hotspot tracks. Liu and Stegman[8] proposed that the CRFB formation resulted from a Miocene slab tear, followed by subsequent hotspot volcanisms caused by plume penetrating the segmented slab. In contrast, Leonard and Liu[19] showed that the slab actually blocks the rising plume and thus prohibits it from generating an extensive surface volcanism. This scenario would certainly become more complex if other lithosphere and mantle processes are further considered. To now, there are no published numerical or analog models that attempt to simulate all these processes simultaneously. Here we present such a system model by taking into account all the major tectonic components.

Hybrid inverse geodynamic modelling

Recent high-resolution tomography images[15,20] beneath continental United States provide an unprecedented opportunity to understand better the past mantle dynamics. These seismic images allow us to reconstruct detailed mantle structures and flow since 20 million years ago (Ma) using a combination of forward modelling[21] and adjoint inversion algorithms[22] (Methods and Zhou and Liu[23] for more details). This hybrid-inversion approach[23] takes advantage of both the accuracy of the seafloor age to define the slab thermal structure[21] and the three-dimensional (3D) configuration of seismic tomography to capture other mantle structures[22], including pre-20 Ma subducted slabs, lithospheric drips and hot-mantle anomalies. Thus, by simultaneously incorporating the detailed plate-motion history, the evolving plate-boundary geometry that accommodates the B&R extension and present-day mantle structures through data assimilation, we formulated a geodynamic model that incorporates all these key tectonic processes for the first time to evaluate quantitatively the mechanism for intraplate volcanism within the western United States.

There are two important model parameters for the hybrid inversion: mantle buoyancy and effective viscosity. The former can be constrained first through the forward simulation[21], in which the prediction of the present-day slab structure (Supplementary Fig. 1) provides a scaling to convert fast seismic anomalies into effective temperatures. We further applied additional constraints on the magnitude of the hot-mantle anomalies from receiver-function analyses[24,25] and petrological inferences[26]. The resulting present-day excess temperature associated with the YS plume represents an upper limit for these independent estimates[24–26] (Methods).

Department of Geology, University of Illinois at Urbana-Champaign, Champaign, IL 61820, USA. *e-mail: qzhou11@illinois.edu

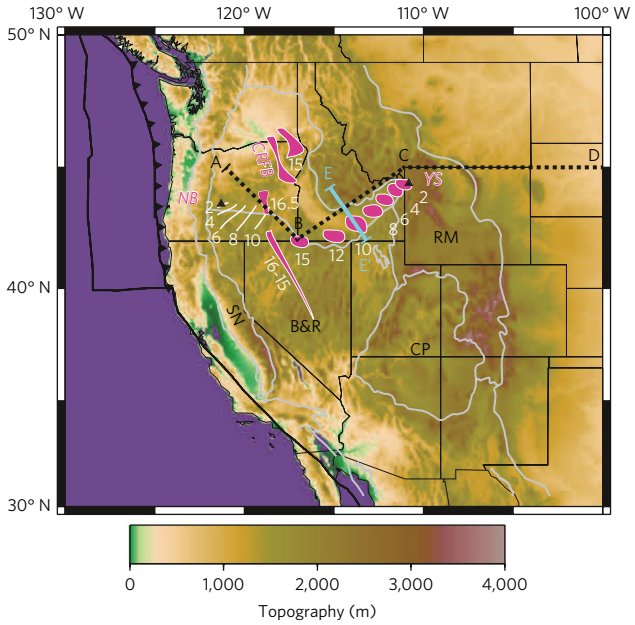

Fig. 1 | Topography of western United States. White contours with a purple interior mark the dyke swarms of the CRFB and the YS hotspot track. Thick white lines mark the NB hotspot track. The profile ABCD shows the map location of the vertical cross-section in Fig. 2. The profile EE′ is the window used to compute the cumulative hot mantle flux below the profile in Fig. 5e. SN, Sierra Nevadal; RM, Rocky Mountains.

Consequently, this allows an estimate of the maximum buoyancy effect of a mantle plume in the formation of surface volcanism. Thus, the estimated thermal state acts as the prediction target of subsequent adjoint iterations[23].

The proper simulation of the Juan de Fuca subduction[21] (Supplementary Fig. 1) with a co-existing YS plume[19] also provides a good constraint on the effective viscosity of the background mantle and that of the slab. The resulting constraint on the temperature dependence of viscosity is applied to estimate the bulk viscosity of the mantle. As the hot anomalies at shallow depths would produce partial melting, we further considered an additional viscosity reduction (to a minimum value of 10^{19} Pa s) of the hot mantle above 200 km depth by enhancing its temperature dependence. In some models, we also applied this viscosity reduction to the plume conduit throughout the entire mantle to test the maximum potential impact of the YS plume.

In practice, we systematically evaluated the buoyancy and viscosity of mantle structures, and important new insights emerge on past mantle dynamics beneath the western United States. These include tracking the evolution of the hot mantle over time, quantifying the various driving forces of mantle flow and evaluating the role of the YS plume during this history.

Evolution of upper mantle hot anomalies

From the reference model, we find that most of the upper-mantle hot anomalies seen in the tomography are derived from the oceanic upper mantle further west (Figs. 2 and 3), instead of from the putative YS plume within the lower mantle. Prior to the mid-Miocene, these hot anomalies are restored to beneath the Juan de Fuca plate. We propose that this hot oceanic asthenosphere (Figs. 2 and 3) represents a northern extension of the hot mantle beneath the Pacific spreading centre, as observed below the East Pacific Rise today[27]. Around 16 Ma, these hot anomalies start to enter the western United States through the central slab tear that forms the CRFB[8] (Figs. 3 and 4). A smaller amount of hot mantle also appears further south, around the slab edge at the Mendocino triple junction (MTJ) (Fig. 4a).

Since the mid-Miocene, hot asthenosphere materials are continually pumped into the western US upper mantle through both the central slab gap and around the MTJ. Subsequently, these hot anomalies are advected further inland to the B&R province and the Snake River Plain (SRP), separated by the thick lithosphere of the Colorado Plateau (CP) and Wyoming Craton (WYC). Meanwhile, these hot anomalies migrate landward around the CP (Figs. 3 and 4). At 70 km depth, within the southern B&R, the hot mantle that has a relatively small temperature anomaly flows east-southeast, and surrounds and encroaches the CP. Further north, the hot mantle with a larger excess temperature advances east-northeast towards the YS caldera and underplates the YS hotspot track (Figs. 2 and 4). From ~8 Ma, the western part of the hot mantle starts to flow backward towards the trench, following the steepening Juan de Fuca slab; this eventually would have formed the NB hotspot track (Figs. 1 and 2). This predicted mantle-flow history is also consistent with the recent inference of pervasive melting below the western United States[28] and the faster-transverse-than-radial seismic anisotropy along the SRP[29,30].

Significantly, the thus-predicted hot-mantle evolution also matches other major volcanic characteristics within the western United States. Prior to 16 Ma, the volcanism in the B&R is predominantly felsic and concentrated towards the Cascadia arc[31], consistent with a hydrated melt source caused by both active subduction along the coast and removal of the earlier flat slab further east[32]. The initial mid-Miocene intrusion and subsequent migration of the hot asthenospheric mantle closely correlate with enhanced mafic volcanism[31,33] across the B&R and along the SRP, both temporally and spatially (Fig. 4). This supports these mafic eruptions being direct asthenospheric melts. In contrast, the correlation between volcanic records and the history of B&R extension is found to be less clear[34]. We refer a quantification of this to future work, because our large-scale model cannot simulate melting associated with crustal extension.

Many local volcanic features could be explained as well. The progressive eastward migration of the hot mantle along the SRP (Figs. 2–4) is consistent with the migrating explosive calderas (Figs. 1 and 4); the widespread hot mantle beneath the SRP since ~8 Ma (Fig. 2) also explains the enduring basaltic volcanism throughout the late Miocene[31] (Fig. 4). That the CP forms a mechanical barrier to the eastward motion of the hot mantle (Figs. 4 and 5) is compatible with the late-Cenozoic encroachment of volcanism towards the CP centre[35,36]. Furthermore, the predicted cumulative volume of hot mantle flowing into the SRP since 10 Ma is about 10^7 km^3 (Fig. 5e), which, assuming a reasonable melt fraction of 5% for the modelled temperature anomaly[37] (Methods), converts into an average magma flux into the crust of about 0.05 km^3 year^{-1}, similar to that inferred from recent petrological estimates[38].

Farralon slab driving hot mantle intrusion

To understand the driving force for the progressive landward migration of hot-mantle anomalies, we analysed the effects of various mantle structures, especially prominent density anomalies that drive flow. Major subcontinental cold anomalies include an upper-mantle downwelling (DW1 in Fig. 2) at the base of the WYC, a lower-mantle anomaly beneath the putative YS plume (DW2 in Fig. 2) and a large-volume downwelling below the eastern United States (DW3 in Fig. 5). Among these, the latter two are generally interpreted as ancient Farallon slabs[12–15], with DW3 being the most voluminous; DW1 is identified less well. Xenolith and xenocryst thermobarometry suggests that continental North America is no thicker than 250 km[39,40], in agreement with inferences from heat flow[41] and receiver-function analysis[42]. Therefore, DW1 might also

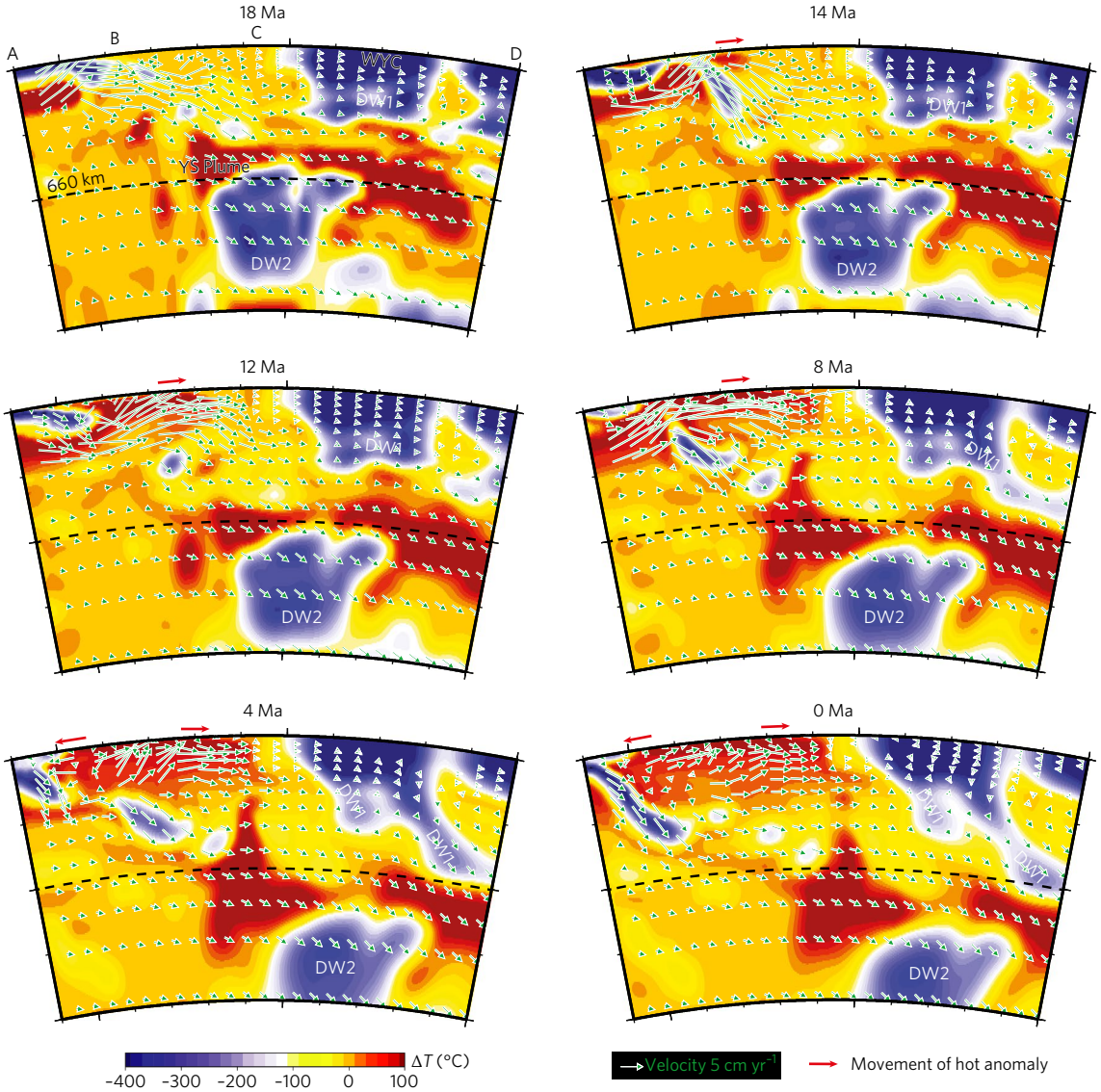

Fig. 2 | Evolution of mantle thermal structures along the NB–YS hotspot tracks from the reference model. a–f, Reconstructed subduction and mantle flow since 18 Ma are shown in the North American reference frame. Red arrows indicate the directions of hot-mantle propagation. The eastward advancing hot mantle and its encroachment into the WYC should have reproduced the time-progressive YS hotspot track. The westward flow above the steepening and retreating Juan de Fuca slab since 8 Ma could explain the NB track. The putative YS plume remains largely covered by the slab and contributes little to the formation of shallow hot anomaly and thus surface volcanism.

represent a former Farallon slab, similar to the interpretation in a recent seismic study[43].

In the reference model (Fig. 2), cold anomalies DW2 and DW3 actively sink and drive the surrounding mantle flow, but DW1 mostly passively drips downward. An additional test (Model A1) with both DW1 and DW2 removed from the initial density structure resulted in a similar mantle flow and distribution of hot anomalies below the western United States (Supplementary Fig. 2a) to those in the reference model (Figs. 2–4). This suggests that DW1 and DW2 play a minor role in driving the large-scale flow. That DW2 does not influence the upper-mantle flow significantly is mostly because of its relatively small volume compared with that of DW3. Consequently, this implies that the ancient Farallon slab beneath the eastern United States (DW3) controls the eastward migration of the hot oceanic asthenosphere and the formation of the YVP and B&R volcanisms. To verify further this dominant role of DW3 in generating intraplate volcanisms, we ran another model (Model A2), in which all the cold-mantle anomalies below 200 km are removed at 20 Ma, but with all hot-mantle anomalies included. The absence of the large-scale downwelling associated with DW3 below the eastern United States means Model A2 generates a much weaker eastward flow beneath the United States (Fig. 5a,b). Consequently, little hot mantle is drawn into the SRP (Fig. 5b,c) and the present-day hot mantle is located mostly to the west of Idaho (Supplementary Fig. 2b), as is controlled by the slab-edge-induced toroidal flow. This difference is also clearly shown in the cumulative mass flux of hot mantle into the SRP as a function of time, for which Model A2 predicts zero flux, in contrast to the progressively increasing flux in the reference model (Fig. 5e). This verifies the dominance of the ancient Farallon slab in driving the eastward flow below YVP.

A third model (Model A3) tests the effect of the lateral pressure gradient that arises from the hot anomalies. Model A3 is the same as the reference model, but the hot anomaly is assumed to be neutrally buoyant. In this case, the hot oceanic asthenosphere passively follows the eastward mantle flow, and the resulting cumulative mass flux of

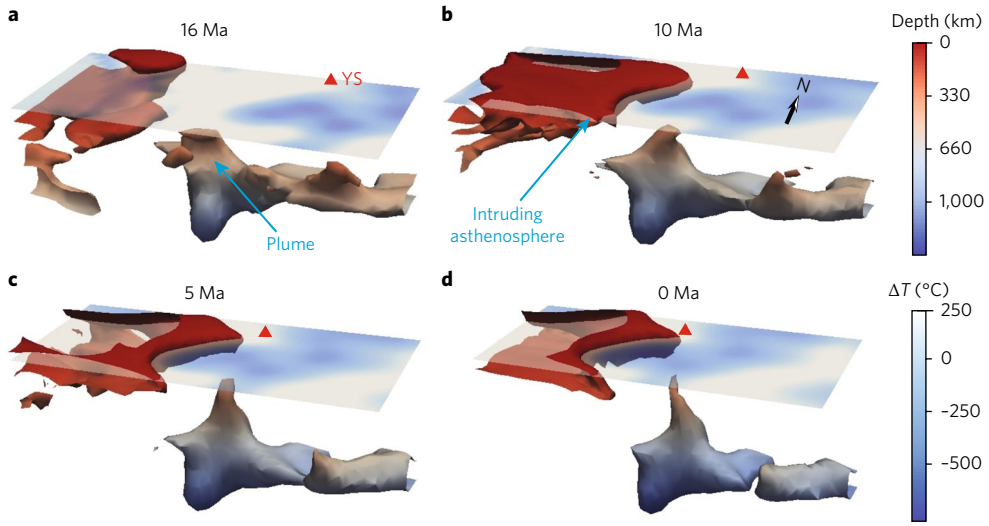

Fig. 3 | 3D representation of mantle evolution in the reference model. a–d, The map area is outlined by the dotted black box in Supplementary Fig. 1a. Both an isosurface (at a temperature of +50 °C relative to the ambient mantle, with colour indicating depth) and the temperature at 60-km depth (the translucent map slice, with colour indicating temperature) are shown. The red triangle marks the location of the present-day YS caldera. At 16 Ma (**a**) most of the hot anomalies are under the oceanic plate, with a first pulse entering the western United States through the slab hole below Oregon that formed the CRFB. Subsequently intruded hot mantle propagates progressively landward toward YS (**b–d**). The plume barely reaches the surface towards the present-day.

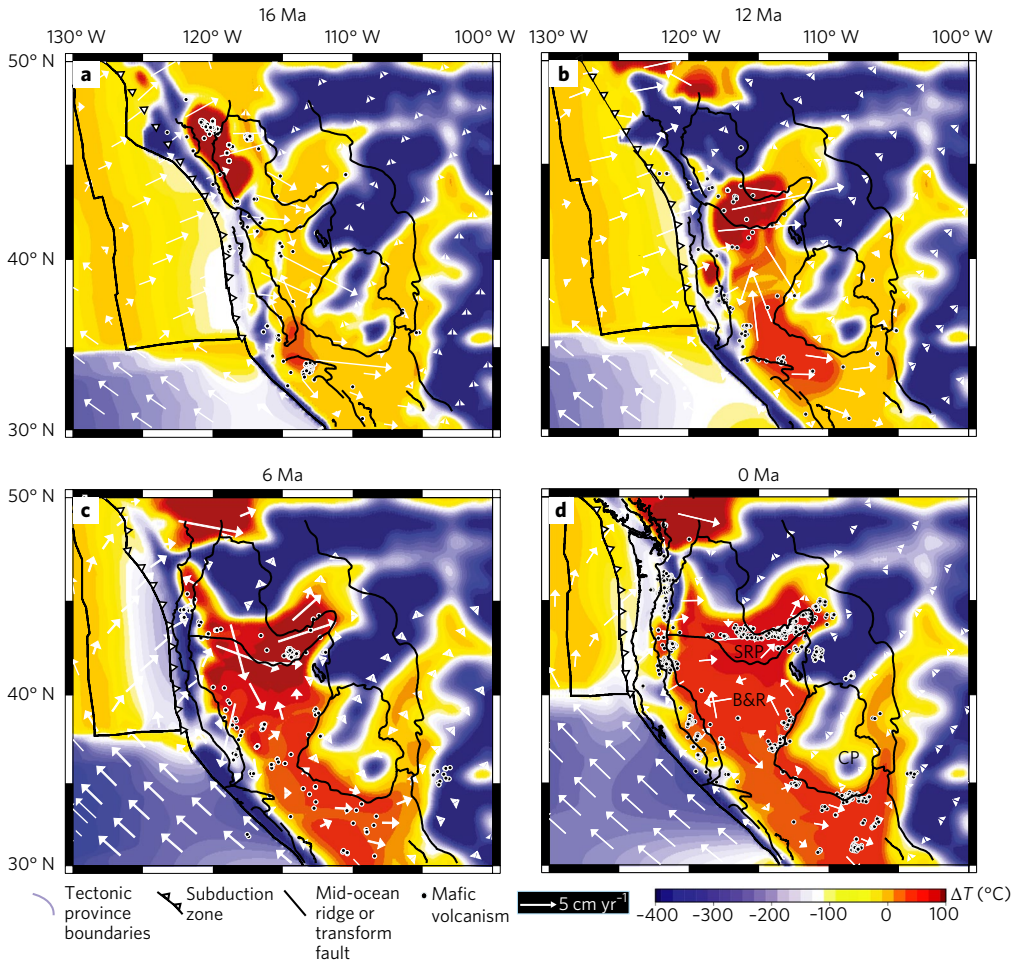

Fig. 4 | Post-CRFB evolution of hot mantle anomalies at 70 km and the history of volcanisms. a–d, Landward intrusion of hot anomalies within the western United States, driven by the sinking of the ancient Farallon slab (DW3) and regulated by lateral lithosphere thickness variations. Their evolution matches the temporal–spatial distribution of basaltic volcanisms within the B&R and the time progression of the NB–YS hotspot tracks. The palinspastically restored volcanic centres and geological provinces are from the literature[31] and the NAVDAT database (www.navdat.org).

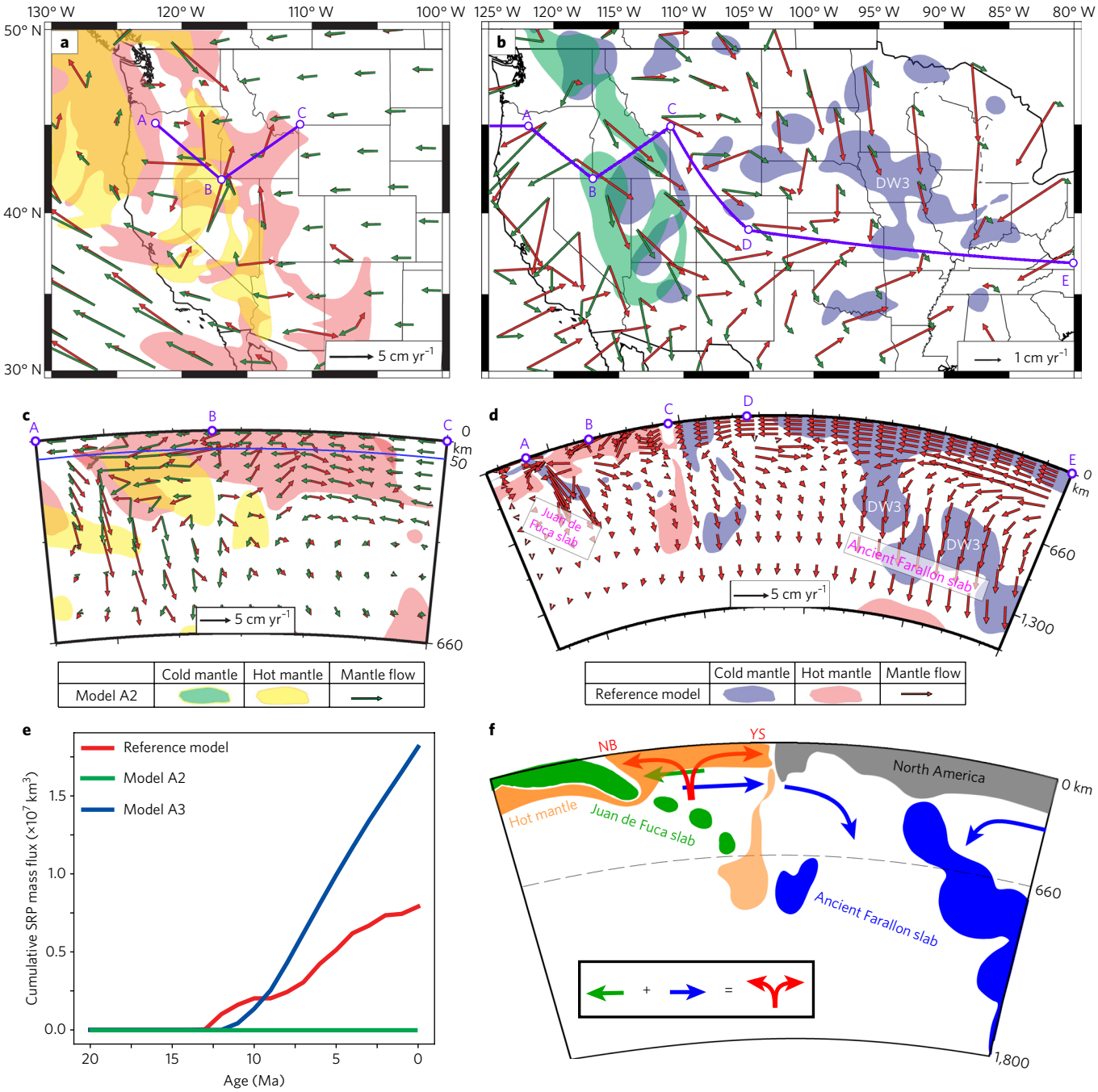

Fig. 5 | Evolution of mantle flow and volcanism in the western United States. a, Mantle flow (arrows) and hot anomaly (contours) at 140 km depth for the reference model and Model A2. The former has large velocity pointing inland and has a hot anomaly reaching the YS. The red arrows are mantle flow velocities for the reference model, the green arrows are velocities for Model A2. The profile ABC is the map location of Fig. 5c. **b**, Mantle flow (arrows) and cold anomaly (contours) at 520-km depth below the entire United States for the two models. The cold anomaly below the western United States is the Juan de Fuca slab, and that below the eastern United States is the top part of the ancient Farallon slab (DW3). In the reference model, mantle flow is drawn towards the ancient Farallon slab; in Model A2, this large-scale eastward mantle flow is missing. The profile ABCDE is the map location of Fig. 5d. **c**, Cross-sectional view along profile ABC in **a**. In the reference model, the velocities below 50-km depth on both sides of point B move away from each other, towards NB and YS, respectively. In Model A2, all velocities move toward NB. **d**, Same as **c**, but for that along profile ABCDE in **b** and only for the reference model. **e**, Cumulative mass flux of hot anomalies into the SRP for the reference Model, Model A2 and Model A3. The reference model and Model A3 have a similar history of mass flux, but Model A2 has zero mass flux. **f**, Sketch of key mantle processes. The ancient Farallon slab (blue) below the eastern United States sinks and drives the eastward mantle below the western United States, whereas the Juan de Fuca slab (green) induces a local westward-returning wedge flow. These two opposing flows generate the YS and NB hotspot tracks.

hot anomalies into the SRP increases even faster over time than in the reference case (Fig. 5e). The predicted present-day hot anomaly is more concentrated along the SRP (Fig. 4d versus Supplementary Fig. 2c) because of the lack of lateral spreading driven by its own buoyancy. The similarity between Model A3 and the reference case suggests that the effective buoyancy of the intruding hot mantle, a

parameter that is not well constrained from observation[24–26], is not crucial for the formation of intraplate volcanism.

Minor role of a YS plume

Although a putative YS plume is frequently invoked in the formation of the YVP[1–4], we do not observe a strong influence of this feature in the regional-scale dynamics. Contrary to the traditional view that a hot plume should ascend because of its own buoyancy, most of the plume volume actually descends with time in our reference model (Figs. 2 and 3). This counterintuitive plume behaviour is caused by a downward viscous entrainment from both the DW2 anomaly underneath and the Juan de Fuca slab above the plume (Fig. 2), a result similar to our recent finding[19]. To explore further the dynamics of the plume, the properties of which are poorly known, we tested several different scenarios. With temperature converted from the original tomography (Model A4) using a scaling directly from the forward model[8,21], the plume continually descends during the entire history, while the intruding hot oceanic asthenosphere still satisfies the volcanic history (Supplementary Figs. 3a–d and 4a–d, and Supplementary Movie 1). With an inflated initial buoyancy of all the hot anomalies (up to +200 °C) and given an open system (that is, volcanism consumes hot anomalies over time), the plume motion is still dominated by the cold anomaly, but could have risen to a depth of ~200 km at the present, as is the case in the reference model (Fig. 2). In this case, the plume has contributed to volcanisms within the eastern SRP close to the present, but its mass flux is too small to account for the widespread slow anomalies observed at shallow depths today. In fact, by removing the entire plume from the model (Model A5), the resulting evolution of the shallow hot mantle remains unchanged (Supplementary Figs. 3e–h and 4e–h, and Supplementary Movie 2), which confirms the negligible role of the plume in providing heat to fuel the YVP. To evaluate the viscosity effects, we used an inflated plume buoyancy and much-reduced plume viscosity (to a minimum of ~10^{19} Pa s) throughout the entire mantle (Supplementary Figs. 5a–d and 6a–d, and Supplementary Movie 3). In this case (Model A6), the plume could reach the surface earlier, but the resulting shallow hot mantle still dominantly originates from the intruding asthenosphere (Supplementary Fig. 5a–d). Another test (Model A7) with all the initial hot anomalies on the oceanic side removed (Supplementary Fig. 5e–h and Supplementary Movie 4) suggests that the plume could rise up to participate in the CRFB, but its subsequent evolution produces a westward instead of eastward moving YS hotspot track (Supplementary Figs. 5e–h and 6e–h, and Supplementary Movie 4). Furthermore, in Models A6 and A7, the YS plume could only produce a very small portion of the observed slow seismic anomalies at the present (Supplementary Fig. 5 and Supplementary Movies 3 and 4). Therefore, according to these models, the plume does not contribute much to the formation of the YVP.

However, one model limitation is the adopted linear rheology, albeit with varying effective viscosity values. With a more-complex nonlinear rheology and melting formulation, it is possible that the plume would behave more dynamically than modelled here, and thus contribute more to the YVP, especially for its geochemical signatures. However, even in that case, we propose that the intrusion of the hot oceanic asthenosphere should still be the dominant process.

Implications on intraplate volcanism formation

By systematically evaluating the post-20 Ma mantle evolution below the western United States, we show that landward intrusion of the hot oceanic asthenosphere represents a robust solution to the formation of intraplate volcanism within the western United States. In this case, a local temperature increase caused by the arrival of hot mantle favours melt formation within both the B&R and YVP. We suggest that the likely presence of volatiles from earlier subduction[32,44] would further reduce the solidus and facilitate volcanism (Methods). In addition, we observe a strong correlation between the eastward migrating hot mantle (Fig. 2) and normal faulting along the SRP[45], which may indicate a resulting lithosphere deformation and/or delamination; if true, this reduction of lithosphere thickness would further enhance local upwelling and partial melting, as recent numerical models demonstrated[46]. Besides the intraplate volcanism, the model also provides potential implications on other observations, such as flow-induced seismic anisotropy and surface uplift (Supplementary Fig. 7), but a detailed discussion is beyond the scope of this paper.

However, we also want to emphasize some model caveats. First, as the model cannot simulate fine-scale processes such as shear-driven upwelling or lithospheric delamination, it requires a pre-existing thinner lithosphere along the SRP, as observed seismically[20,42], to have focused hot anomalies and thus formed localized volcanisms[46]. Second, although a smaller volume of hot anomalies also swept through the B&R, there was much-less accompanying volcanism in this region (Fig. 4). This is probably because the B&R has a broad, thin lithosphere (~60 km)[42], whose lack of lateral lithospheric thickness variation prohibits local upwelling and melting.

We argue that, mechanically, the sinking of the ancient Farallon slab below the eastern United States exerts a dominant control on the eastward intrusion of hot mantle below the YVP, the B&R and the CP (Fig. 5d,f). The returning wedge flow above the subducting Juan de Fuca plate and the toroidal flow around slab edges only affect near-arc processes, such as the westward-moving NB track, since 8 Ma (Fig. 5d,f). We propose that other factors, such as the buoyancy of the shallow hot anomalies and that of a deeper plume, play a secondary role in controlling mantle flow, in contrast with the popular view that the plume is the main driver of the YS volcanic system. However, the plume may behave more dynamically in a model that incorporates a more-realistic rheology that brings in more deep-mantle materials to formulate the geochemical properties. We suggest that our mechanism of intraplate volcanism formation may apply to other similar tectonic environments as well.

Methods

Methods, including statements of data availability and any associated accession codes and references, are available at https://doi.org/10.1038/s41561-017-0035-y.

Received: 16 August 2017; Accepted: 22 November 2017;
Published online: 18 December 2017

References

1. Pierce, K. L. & Morgan, L. A. The track of the Yellowstone hot spot: volcanism, faulting, and uplift. *Geol. Soc. Am. Mem.* **179**, 1–54 (1992).
2. Camp, V. E. & Ross, M. E. Mantle dynamics and genesis of mafic magmatism in the intermontane Pacific Northwest. *J. Geophys. Res.* **109**, B8 (2004).
3. Smith, R. B., Jordan, M., Steinberger, B., Puskas, C. M., Farrell, J., Waite, G. P., Husen, S., Chang, W. L. & O'Connell, R. Geodynamics of the Yellowstone hotspot and mantle plume: seismic and GPS imaging, kinematics, and mantle flow. *J. Volcanol. Geoth. Res.* **188**, 26–56 (2009).
4. Kincaid, C., Druken, K. A., Griffiths, R. W. & Stegman, D. R. Bifurcation of the Yellowstone plume driven by subduction-induced mantle flow. *Nat. Geosci.* **6**, 395–399 (2013).
5. Carlson, R. W. & Hart, W. K. Crustal genesis on the Oregon plateau. *J. Geophys. Res.* **92**, 6191–6206 (1987).
6. Christiansen, R. L., Foulger, G. R. & Evans, J. R. Upper-mantle origin of the Yellowstone hotspot. *Geol. Soc. Am. Bull.* **114**, 1245–1256 (2002).
7. James, D., Fouch, M., Carlson, R. & Roth, J. Slab fragmentation, edge flow and the origin of the Yellowstone hotspot track. *Earth Planet. Sci. Lett.* **311**, 124–135 (2011).
8. Liu, L. & Stegman, D. R. Origin of the Columbia River flood basalt controlled by propagating rupture of the Farallon slab. *Nature* **482**, 386–390 (2012).
9. King, S. D. & Anderson, D. L. Edge-driven convection. *Earth Planet. Sci. Lett.* **160**, 289–296 (1998).
10. Hales, T. C., Abt, D. L., Humphreys, E. D. & Roering, J. J. A lithospheric instability origin for Columbia River Flood Basalts and Wallowa Mountains uplift in northeast Oregon. *Nature* **438**, 842–845 (2005).

11. Seton, M., Müller, R. D., Zahirovic, S., Gaina, C., Torsvik, T., Shephard, G., Talsma, A., Gurnis, M., Turner, M. & Chandler, M. Global continental and ocean basin reconstructions since 200 Ma. *Earth-Science Rev.* **113**, 212–270 (2012).
12. van der Hilst, R. D., Widiyantoro, S. & Engdahl, E. R. Evidence of deep mantle circulation from global tomography. *Nature* **386**, 578–584 (1997).
13. Grand, S. P. Mantle shear-wave tomography and the fate of subducted slabs. *Phil. Trans. R. Soc. Lond. A* **360**, 2475–2491 (2002).
14. Ren, Y., Stutzmann, E., van Der Hilst, R. D. & Besse, J. Understanding seismic heterogeneities in the lower mantle beneath the Americas from seismic tomography and plate tectonic history. *J. Geophys. Res.* **112**, B004154 (2007).
15. Sigloch, K. Mantle provinces under North America from multifrequency *P* wave tomography. *Geochem. Geophys. Geosyst.* **12**, Q02W08 (2011).
16. van der Meer, D. G., Spakman, W., Van Hinsbergen, D. J. J., Amaru, M. L. & Torsvik, T. H. Towards absolute plate motions constrained by lower-mantle slab remnants. *Nat. Geosci.* **3**, 36–40 (2010).
17. Müller, R. D., Sdrolias, M., Gaina, C., Steinberger, B. & Heine, C. Long-term sea-level fluctuations driven by ocean basin dynamics. *Science* **319**, 1357–1362 (2008).
18. Liu, L. The ups and downs of North America: evaluating the role of mantle dynamic topography since the Mesozoic. *Rev. Geophys.* **53**, 1022–1049 (2015).
19. Leonard, T. & Liu, L. The role of a mantle plume in the formation of Yellowstone volcanism. *Geophys. Res. Lett.* **43**, 1132–1139 (2016).
20. Schmandt, B. & Lin, F. C. P & S wave tomography of the mantle beneath the United States. *Geophys. Res. Lett.* **41**, 6342–6349 (2014).
21. Liu, L. & Stegman, D. R. Segmentation of the Farallon slab. *Earth Planet. Sci. Lett.* **311**, 1–10 (2011).
22. Liu, L. & Gurnis, M. Simultaneous inversion of mantle properties and initial conditions using an adjoint of mantle convection. *J. Geophys. Res.* **113**, B08405 (2008).
23. Zhou, Q. & Liu, L. A hybrid approach to data assimilation for reconstructing the evolution of mantle dynamics. *Geochem. Geophys. Geosyst.* **18**, C007116 (2017).
24. Schmandt, B., Dueker, K. G., Humphreys, E. D. & Hansen, S. H. Hot mantle upwelling across the 660 beneath Yellowstone. *Earth Planet. Sci. Lett.* **331–332**, 224–236 (2012).
25. Gao, S. S. & Liu, K. H. Mantle transition zone discontinuities beneath the contiguous United States. *J. Geophys. Res.* **119**, 6452–6468 (2015).
26. Leeman, W. P., Schutt, D. L. & Hughes, S. S. Thermal structure beneath the Snake River Plain: implications for the Yellowstone hotspot. *J. Volcanol. Geoth. Res.* **188**, 57–67 (2009).
27. Ritsema, J., Deuss, A., van Heijst, H. J. & Woodhouse, J. H. S40RTS: a degree-40 shear-velocity model for the mantle from new Rayleigh wave dispersion, teleseismic traveltime and normal-mode splitting function measurements. *Geophys. J. Int.* **184**, 1223–1236 (2011).
28. Hier-Majumder, S. & Tauzin, B. Pervasive upper mantle melting beneath the western US. *Earth Planet. Sci. Lett.* **463**, 25–35 (2017).
29. Bozdağ, E., Peter, D., Lefebvre, M., Komatitsch, D., Tromp, J., Hill, J., Podhorszki, N. & Pugmire, D. Global adjoint tomography: first-generation model. *Geophys. J. Int.* **207**, 1739–1766 (2106).
30. Huang, Z. & Zhao, D. Mapping *P*-wave azimuthal anisotropy in the crust and upper mantle beneath the United States. *Phys. Earth Planet. Int.* **225**, 28–40 (2013).
31. McQuarrie, N. & Wernicke, B. P. An animated tectonic reconstruction of southwestern North America since 36 Ma. *Geosphere* **1**, 147–172 (2005).
32. Humphreys, E. D. Post-Laramide removal of the Farallon slab, western United States. *Geology* **23**, 987–990 (1995).
33. DePaolo, D. J. & Daley, E. E. Neodymium isotopes in basalts of the southwest basin and range and lithospheric thinning during continental extension. *Chem. Geol.* **169**, 157–185 (2000).
34. Gans, P. B. & Bohrson, W. A. Suppression of volcanism during rapid extension in the Basin and Range Province, United States. *Science* **279**, 66–68 (1998).
35. Roy, M., Jordan, T. H. & Pederson, J. Colorado Plateau magmatism and uplift by warming of heterogeneous lithosphere. *Nature* **459**, 978–982 (2009).
36. Reid, M. R., Bouchet, R. A., Blichert-Toft, J., Levander, A., Liu, K., Miller, M. S. & Ramos, F. C. Melting under the Colorado Plateau, USA. *Geology* **40**, 387–390 (2012).
37. Katz, R. F., Spiegelman, M. & Langmuir, C. H. A new parameterization of hydrous mantle melting. *Geochem. Geophys. Geosyst.* **4**, 1073 (2003).
38. McCurry, M. & Rodgers, D. W. Mass transfer along the Yellowstone hotspot track I: petrologic constraints on the volume of mantle-derived magma. *J. Volcanol. Geotherm. Res.* **188**, 86–98 (2009).
39. Carlson, R. W., Pearson, D. G. & James, D. E. Physical, chemical, and chronological characteristics of continental mantle. *Rev. Geophys.* **43**, RG1001 (2005).
40. Griffin, W. L., O'Reilly, S. Y., Doyle, B. J., Pearson, N. J., Coopersmith, H., Kivi, K. & Pokhilenko, N. Lithosphere mapping beneath the North American plate. *Lithosphere* **77**, 873–922 (2004).
41. Mareschal, J. C. & Jaupart, C. Variations of surface heat flow and lithospheric thermal structure beneath the North American craton. *Earth Planet. Sci. Lett.* **223**, 65–77 (2004).
42. Hansen, S. M., Dueker, K. & Schmandt, B. Thermal classification of lithospheric discontinuities beneath USArray. *Earth Planet. Sci. Lett.* **431**, 36–47 (2015).
43. Humphreys, E. D., Schmandt, B., Bezada, M. J. & Perry-Houts, J. Recent craton growth by slab stacking beneath Wyoming. *Earth Planet. Sci. Lett.* **429**, 170–180 (2015).
44. Gerya, T. V., Yuen, D. A. & Sevre, E. O. D. Dynamic causes for incipient magma chambers above slabs. *Geology* **32**, 89–92 (2004).
45. Rodgers, D.W., Ore, H. T., Bobo, R. T., McQuarrie, N. & Zentner, N. in *Tectonic and Magmatic Evolution of the Snake River Plain Volcanic Province* (eds Bonnichsen, B., White, C. M. & McCurry, M.) 121–155 (Bulletin 30, Idaho Geological Survey, Moscow, 2002).
46. Ballmer, M. D., Conrad, C. P., Smith, E. I. & Johnsen, R. Intraplate volcanism at the edges of the Colorado Plateau sustained by a combination of triggered edge-driven convection and shear-driven upwelling. *Geochem. Geophys. Geosyst.* **16**, 366–379 (2015).

Acknowledgements

The numerical models were performed using CitcomS (www.geodynamics.org) and GPlates (www.gplates.org). Figures were prepared using the GMT software package (https://www.soest.hawaii.edu/gmt/). This work is supported by National Science Foundation grant EAR-1345135, EAR-1554554. This research is part of the Blue Waters sustained-petascale computing project, which is supported by the National Science Foundation (awards OCI-0725070 and ACI-1238993) and the state of Illinois. Blue Waters is a joint effort of the University of Illinois at Urbana-Champaign and its National Center for Supercomputing Applications. This work is also part of the "PRAC Title 4-D Geodynamic Modeling With Data Assimilation: Origin Of Intra-Plate Volcanism In The Pacific Northwest" PRAC allocation support by the National Science Foundation (award number ACI 1516586). This work also used the Extreme Science and Engineering Discovery Environment (XSEDE), which is supported by National Science Foundation grant number ACI-1548562.

Author contribution

Q.Z. carried out all the numerical simulations. L.L. designed and oversaw the project. Both Q.Z. and L.L. contributed to the results interpretation and manuscript preparation. J.H. contributed to the figure preparation.

Competing financial interests

The authors declare no competing financial interests.

Additional information

Supplementary information is available for this paper at https://doi.org/10.1038/s41561-017-0035-y.

Reprints and permissions information is available at www.nature.com/reprints.

Correspondence and requests for materials should be addressed to Q.Z.

Publisher's note: Springer Nature remains neutral with regard to jurisdictional claims in published maps and institutional affiliations.

Methods

Supplementary Online Information and Zhou and Liu[23] for additional details of the numerical model, including governing equations, rheology and model set-up.

Hybrid forward and adjoint data assimilation algorithms. To take advantage of both the high-resolution forward simulation and the comprehensive mantle structures from the adjoint simulation, we designed a hybrid simulation approach. On the one hand, we perform a forward subduction model[21] that starts from 40 Ma and terminates at 20 Ma. On the other hand, we estimate the 20 Ma mantle structure based on tomography using a simple backward integration[22]. Subsequently, we introduce the adjoint algorithm to match the current mantle seismic structures further through additional forward-adjoint iterations. Features that are reproduced successfully via this hybrid approach include the actively subducting Juan de Fuca slab, fast seismic anomalies associated with the continental lithosphere and those at greater depths to the east of the western United States, as well as the widespread slow anomalies within both the upper and lower mantle (Supplementary Fig. 1).

During the adjoint inversion back to 20 Ma, we iteratively update the initial mantle structure, but without updating the actively subducting slab above 200 km. This way, we preserve in the present-day mantle both the post-20 Ma slab and mantle structures not derived from this subduction history[23] (Supplementary Information). Eventually, the model reproduces the evolution of both slab- and lithosphere-related fast seismic anomalies and the hot-mantle-related slow anomalies. We emphasize that because of the hybrid nature of this inversion and the higher accuracy of the seafloor age for defining slab geometry than the seismic image, we do not force the present-day mantle to match the tomography at every detail. Instead, we look for a model that satisfies the exact seafloor-age constraint (reflected in the forwardly predicted slab configuration) and the overall pattern (at a wavelength jointly determined by the slab and tomography) of other seismic anomalies at the present day (Fig. 1 and Supplementary Fig. 1).

We point out one potential caveat of this inversion: early volcanic processes that occur close to the subduction zone, such as the CRFB, are non-recoverable, because the hot mantle that triggers these volcanisms has largely disappeared today through both high-degree eruption back then and subsequent slab entrainment. In fact, the current lithosphere around the CRFB is seismically fast, and was interpreted as cold residual mantle because of the excessive extraction of melt during CRFB formation and/or accreted Farallon slab[42]. We adopt this scenario in our model by postponing the assimilation of the cold lithosphere from tomography within eastern Oregon to one million years after the CRFB formation. Furthermore, we also parameterize a hot mantle region that was initially beneath the Farallon plate offshore Oregon, at latitude 42–45° and longitude 237.5–248°, at 20 Ma. Tests show that this extra-hot mantle is required to help with the flood-basalt formation at 16 Ma, as well as to better match the lower mantle slab geometry today, validating this model assumption. This parameterization means we could not test the proposed lithosphere delamination associated with the CRFB[47], as well as the subsequent volcanic history in its nearby region.

Estimating the reference present-day mantle temperature field. We convert seismic velocity anomalies from recent tomography images[15,20] into temperature perturbations. A detailed seismic structure for the mantle down to a 1,200 km depth beneath the United States is available[20], but that beyond is missing. As the mantle beneath the Juan de Fuca plate is also important to understand convection beneath the continent, we expanded these mantle structures[20] further into the surrounding oceanic parts and also down to the core–mantle boundary using a larger-scale regional tomography[15] (Supplementary Fig. 1). There is a mismatch between the references of the models of Sigloch[15] and Schmandt and Lin[20]. We first compute the average seismic velocity anomaly of the two models for each depth, and then shift the larger-scale one[15] using the difference so that they have the same baseline. With the thus-corrected tomography images for the region right below the continent down to 1,200 km, we directly adopt the seismic model[20]. Beyond this region, we adopt the larger-scale model[15], and a gradual transition function merges the two models along the edges. This composite tomography image provides a physically adequate reference state for mantle evolution beneath the western United States since 20 Ma.

We also consider natural complexities during the seismic-to-temperature conversion. On the one hand, the strongest slow seismic anomalies (as large as −8%) are mostly located beneath active volcanic regions, such as YS, and recent studies suggest that slow anomalies with magnitudes larger than 5% are probably result from partial melt[48]. On the other hand, extreme values of fast seismic anomalies are usually found in the cratonic lithosphere, whose seismic properties are compositionally controlled. Therefore, we discarded the extreme values of seismic anomalies, and applied a scaling such that fast anomalies below 4% are linearly converted into temperature anomalies of −700 to 0 °C, and slow anomalies below 3% are linearly converted into 0–200 °C. The low temperatures are consistent with the thermal structure of the forward predicted slabs[21]. The high temperatures correspond to a maximum estimate of excess temperature of the sub-YS mantle plume[24–26].

On the melt fraction of hot oceanic asthenosphere below SRP. We have compared our modelled temperature anomaly with the required temperature for a 5% melt fraction[37,49–51], a value we assume in the main text. At 4 GPa, the solidus for dry peridotite ranges from 1,520 °C to 1,650 °C (refs [37,49]). Our inferred temperature anomaly is 100–150 °C more than the ambient mantle temperature. If the potential temperature for mid-ocean ridge basalt petrogenesis is 1,430 °C[50], then our modelled hot anomaly is 1,570–1,620 °C (given a 0.4 °C km^{-1} adiabatic temperature gradient), falling in the range of the solidus for dry peridotite. Moreover, when water or CO_2 is added, a reasonable assumption for the oceanic asthenosphere and a very likely scenario for a mantle wedge, the solidus of peridotite can be depressed by more than 100 °C[37,50]. From an early study[51], it is suggested that for peridotites with 0.01% water, a 5% melt requires 1,380 °C at the asthenosphere depth. More-recent studies also suggest that 5% melt below the lithosphere is likely with water or CO_2 present and with a temperature anomaly of +100 °C relative to the ambient mantle[37,50]. As the western United States has experienced prolonged subduction since the Mesozoic and, in particular, an extensive flat slab existed prior to 20 Ma, a considerable amount of water is likely to be present throughout the upper mantle of the SRP. As a result, when the hot oceanic asthenosphere swept through the region, the pre-existing water could catalyse melting. Therefore, we think a 5% melt fraction beneath the SRP is a possible scenario.

Code availability. The original version of the code used to simulate mantle convection can be accessed at www.geodynamics.org/cig/software/citcoms/. The code used to generate plate-motion data can be accessed at www.gplates.org. The code used to make the figures can be accessed at www.soest.hawaii.edu/gmt/ and www.paraview.org/.

Data availability. The tomography data that supports the findings of this study in Schmandt and Lin[20] can be accessed at www.ds.iris.edu/ds/products/emc-us-sl-2014/, and the tomography data in Sigloch[15] are available within that paper and its supporting information. The volcanic data can be accessed at www.navdat.org.

References

47. Darold, A. & Humphreys, E. D. Upper mantle seismic structure beneath the Pacific Northwest: A plume-triggered delamination origin for the Columbia River flood basalt eruptions. *Earth Planet. Sci. Lett.* **365**, 232–242 (2013).
48. Huang, H. H., Lin, F. C., Schmandt, B., Farrell, J., Smith, R. B. & Tsai, V. C. The Yellowstone magmatic system from the mantle plume to the upper crust. *Science* **348**, 773–776 (2015).
49. Asahara, Y. & Ohtani, E. Melting relations of the hydrous primitive mantle in the CMAS–H_2O system at high pressures and temperatures, and implications for generation of komatiites. *Phys. Earth Planet. Inter.* **125**, 31–44 (2011).
50. Green, D. H. Experimental petrology of peridotites, including effects of water and carbon on melting in the Earth's upper mantle. *Phys. Chem. Minerals* **42**, 95–122 (2015).
51. Green, D. H. & O'Hara, M. J. Composition of basaltic magmas as indicators of conditions of origin: application to oceanic volcanism. *Phil. Trans. R. Soc. A* **268**, 707–725 (1971).